

Giant dipole resonance in deformed nuclei: dependence on Skyrme forces

V.O. Nesterenko, W. Kleinig *

*Laboratory of Theoretical Physics, Joint Institute for Nuclear Research,
Dubna, Moscow region, 141980, Russia
nester@theor.jinr.ru; kleinig@theor.jinr.ru*

J. Kvasil, P. Vesely

*Institute of Particle and Nuclear Physics,
Charles University, CZ-18000 Praha, Czech Republic
kvasil@ipnp.troja.mff.cuni.cz; vesely@ipnp.troja.mff.cuni.cz*

P.-G. Reinhard

*Institut für Theoretische Physik II,
Universität Erlangen, D-91058, Erlangen, Germany;
mpt218@theorie2.physik.uni-erlangen.de*

(Dated: October 21, 2018)

Abstract

The giant dipole resonance (GDR) in deformed nuclei is analyzed using the self-consistent separable random-phase-approximation (SRPA) with Skyrme forces SkT6, SkM*, SLy6 and SkI3. The deformed nuclei ^{150}Nd and ^{238}U are used as representative rare-earth and actinide samples. Dependencies of the dipole strength distributions on some basic characteristics of the Skyrme functional and nuclear matter properties (isoscalar and isovector effective masses, time-odd contributions) are discussed. Particular attention is paid to the fragmentation structure of the GDR strength which are shown to depend sensitively to spin-orbit intruder states with large angular momentum.

PACS numbers: 21.30.Fe, 21.60.Ev, 21.60.Jz

* Permanent address: Technische Universität Dresden, Inst. für Analysis, D-01062, Dresden, Germany

I. INTRODUCTION

Skyrme forces [1, 2, 3, 4] are widely used for the self-consistent description of ground state and excitations of atomic nuclei (for a recent review see [5]). Recently, there is increasing interest in applications to the dynamics of exotic deformed nuclei, see e.g. [6, 7, 8]. The demands on the reliability and quality of the description are higher now than in the pioneering earlier studies. This calls for closer inspection of the dynamical properties of Skyrme forces. For example, there are still several open problems related to the description of giant resonances, particularly for the for isovector modes [9], for which the giant dipole resonance (GDR) is the most prominent representative. Already for the description of the GDR, there still exist a several puzzling features. For example, some trends of GDR properties with nuclear matter characteristics look at first glance surprising (microscopic calculations [9] show a decrease of the GDR energy with increasing symmetry energy while macroscopic estimates predict the opposite trend [10]). Another puzzling feature is that some Skyrme parameterizations (like SkM*) yield a too large high-energy shoulder of the dipole strength distribution in heavy nuclei [8, 11]. Moreover, the influence of the effective mass and related time-odd couplings in the Skyrme forces on the GDR spectra has not yet been fully clarified and deserves closer inspection. The aim of this contribution is to explore more closely these GDR properties in heavy deformed nuclei.

Until recently, the treatment of excitations in deformed nuclei within self-consistent models was rather involved and time consuming. Meanwhile, a new generation of the efficient RPA schemes has emerged [6, 7, 11, 12, 13], which allow now the systematic studies. In this contribution, we will exploit one of these schemes, the separable random-phase-approximation (SRPA). This method drastically simplifies the calculations and, at the same time, provides high accuracy. It can be used for both spherical [11] and deformed [12, 13] nuclei. Here we will apply it to study trends and spectral pattern of the GDR in heavy deformed nuclei ^{150}Nd and ^{238}U . Descriptions for four different Skyrme forces will be compared and scrutinized.

TABLE I: Nuclear matter and deformation properties for the Skyrme forces under consideration. The table represents the isoscalar effective mass m_0^*/m , symmetry energy a_{sym} , density dependence of symmetry energy $a'_{\text{sym}} = d/d\rho a_{\text{sym}}$, sum rule enhancement factor κ , isovector effective mass $m_1^*/m = 1/(1 + \kappa)$, and quadrupole moments Q_2 in ^{150}Nd and ^{238}U . The experimental values of Q_2 are taken from [19].

Forces	m_0^*/m	a_{sym} [MeV]	a'_{sym} [MeV fm ³]	κ	m_1^*/m	Q_2 [b]	
						^{150}Nd	^{238}U
SkT6	1.00	30.0	63	0.001	1.00	6.0	11.1
SKI*	0.79	30.0	95	0.531	0.65	6.2	11.1
SLy6	0.69	32.0	100	0.250	0.80	5.8	11.0
SkI3	0.58	34.8	212	0.246	0.80	5.9	11.0
exp.						5.2	11.1

II. DETAILS OF CALCULATIONS

The explicit form of the Skyrme functional used in our study is given elsewhere [11, 14]. The calculations are performed for the Skyrme forces SkT6 [15], SkM* [16], SLy6 [17] and SkI3 [18]. Though these forces were fitted with a different bias, they all provide a good overall description of nuclear bulk properties and are suitable for deformed nuclei (see review [5]). For our aim it is important that this selection of forces covers different values of key characteristics of nuclear matter, as shown in Table 1. We so dispose a large span of the effective masses (isoscalar as well as isovector) and some variation of the symmetry energy.

The calculations employ a cylindrical coordinate-space grid with the mesh size 0.7 fm. Pairing is treated at the BCS level. The ground state deformation is determined by minimizing the total energy. As is seen from Table 1, all three Skyrme forces give a reasonable quadrupole moment in ^{238}U . The calculated moment in ^{150}Nd is somewhat overestimated. However, this nucleus is rather soft and it is difficult to expect here a precise agreement with the experiment. The modest overestimation is not a principle obstacle for our study.

The dipole response involves contributions from both time-even (nucleon ρ_s , kinetic energy τ_s , and spin-orbital \mathfrak{S}_s) and time-odd (current j_s and spin σ_s) densities, where s denotes protons and neutrons. Besides, the contributions from the pairing densities χ_s is taken into

account. The contributions of the time-odd densities are driven by the variations

$$\frac{\delta^2 E}{\delta \vec{j}_{s1} \delta \vec{j}_s}, \quad \frac{\delta^2 E}{\delta \vec{\sigma}_{s1} \delta \vec{j}_s}, \quad \frac{\delta^2 E}{\delta \vec{j}_{s1} \delta \vec{\sigma}_s} \quad (1)$$

of the Skyrme functional terms [11, 14]

$$\begin{aligned} & b_1(\rho\tau - \vec{j}^2) - b'_1 \sum_s (\rho_s \tau_s - \vec{j}_s^2) \\ & - b_4 \left(\rho(\vec{\nabla} \cdot \vec{\sigma}) + \vec{\sigma} \cdot (\vec{\nabla} \times \vec{j}) \right) - b'_4 \sum_s \left(\rho_s(\vec{\nabla} \cdot \vec{\sigma}_s) + \vec{\sigma}_s \cdot (\vec{\nabla} \times \vec{j}_s) \right) \end{aligned} \quad (2)$$

where the total densities (like $j = j_p + j_n$) are given without the index. As was shown in refs. [3, 4], the time-odd densities naturally belong to the Skyrme functional if it involves all the possible bilinear combinations of the nucleon and spin densities together with their derivatives up to the second order. The time-odd densities enter the functional only in specific combinations, as a complement to the time-even ones, so as to keep Galilean and gauge invariance of Skyrme forces.

The present SRPA calculations are performed in the approximation of two generating operators, which allows to cover dynamics in both surface and interior of the nucleus [12]. The dipole response is computed as the photo-absorption energy-weighted strength function

$$S(E\lambda\mu; \omega) = \sum_{\nu} \omega_{\nu} M_{\lambda\mu\nu}^2 \zeta(\omega - \omega_{\nu}) \quad (3)$$

where

$$\zeta(\omega - \omega_{\nu}) = \frac{1}{2\pi} \frac{\Delta}{(\omega - \omega_{\nu})^2 + (\Delta/2)^2} \quad (4)$$

is the Lorentz weight with the averaging parameter Δ , $M_{\lambda\mu\nu}$ is the matrix element of $E\lambda\mu$ transition from the ground state to the RPA state $|\nu\rangle$, ω_{ν} is the RPA eigen-energy. By using the SRPA technique [12, 13], we directly compute the strength function with the Lorentz weight. This dramatically reduces the computation time. For example, by using a PC with CPU Pentium 4 (3.0 GHz) we need about 25 minutes for the complete calculations of the GDR in ^{238}U .

The isovector dipole response is computed with the proton and neutron effective charges $e_p^{eff} = N/A$ and $e_n^{eff} = -Z/A$, where Z , N are numbers of protons and neutrons and A is the mass number. The isoscalar spurious mode (center of mass) is located at 2-3 MeV and thus is safely separated from the isovector one. We use a large configuration

space including all proton and neutron levels from the bottom of the potential well up to $\sim +16$ MeV. This results in ~ 7300 (^{150}Nd) and ~ 9500 (^{238}U) two-quasiparticle (2QP) configurations in the energy interval 0 - 100 MeV. In both nuclei, the energy-weighted sum rule $EWSR = 9NZ\hbar^2e^2/(8A\pi m^*)$ is exhausted by 99%, 97%, 93%, and 89% for SkT6, SkM*, SLy6, and SkI3 forces, respectively.

III. RESULTS AND DISCUSSION

Results of the calculations are presented in Figs. 1-3.

Figure 1 exhibits the results for the dipole strength computed with a width parameter $\Delta = 2$ MeV. This width is supposed to simulate line broadening from nucleon escape as well as two-body collisions and it is found to be suitable for the comparison with the experimental data. For comparison, we show also the unperturbed dipole strength deduced from the pure two-quasi-particle (2qp) excitations.

The figure shows a strong dependence of the dipole response on the Skyrme forces. This dependence is particularly pronounced for the unperturbed strength where it is obviously related to the isoscalar effective mass m_0^*/m . Low effective masses yield a stretched single particle spectrum (see e.g. [20]) leading to large 2qp energies. Following this trend, the unperturbed 2qp strength in Fig. 1 exhibits a systematic shift to higher energy from SkT6 to SkI3.

The residual interaction in the isovector dipole channel is repulsive and moves the dipole strength to higher energies. The corresponding collective energy shift is determined by the isovector parameters listed in Table 1. What is remarkable, there is a clear correlation in the dependencies of the 2qp strength and the collective shift on the Skyrme force. The dependencies are opposite. A small effective mass m_0^*/m stretches the 2qp spectrum and, at the same time, we have reduction of the residual interaction driven by m_1^*/m . Thereby, both effective masses contribute and maybe even correlate. The latter might be justified by that both effective masses originate from one and the same term of the Skyrme functional $\sim b_1, b_1'$. After all, we obtain similar GDR energies for all the forces, in fair agreement with the experimental data [21, 22]. These results corroborate the experience from spherical nuclei that SRPA with Skyrme forces provides a reasonable description of the GDR in heavy nuclei [11].

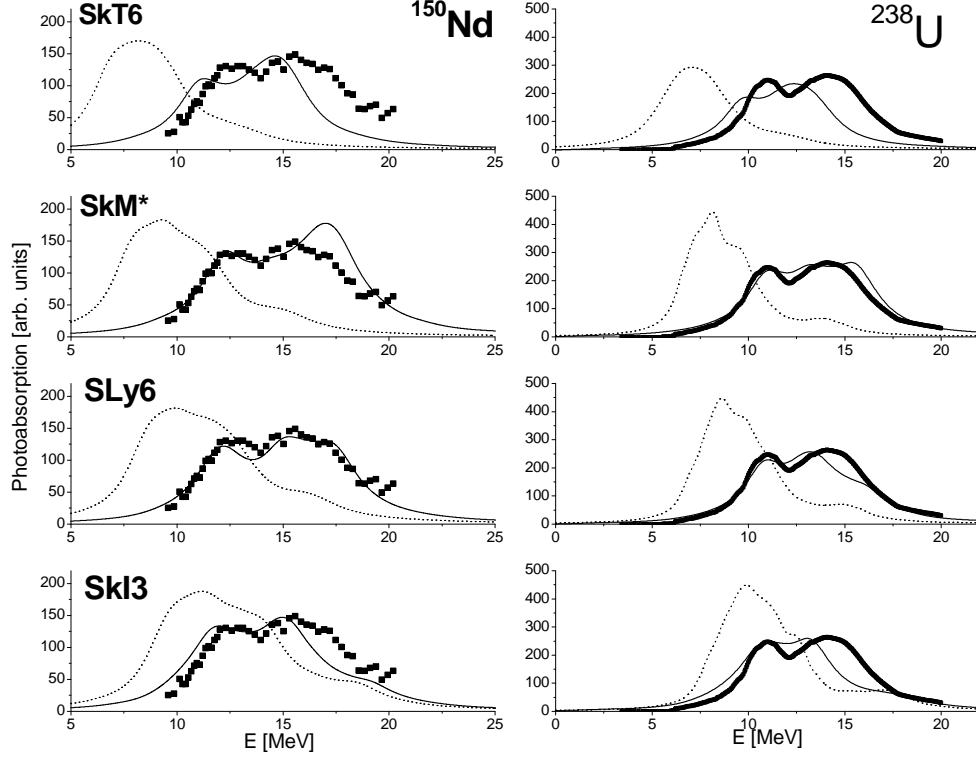


FIG. 1: The dipole giant resonance in ^{150}Nd and ^{238}U , calculated with the Skyrme forces SkT6, SkM*, SLy6 and SkI3. The calculated strength (solid curve) is compared with the experimental data [21, 22] (triangles). The quasiparticle (unperturbed) strength is denoted by the dotted curve. The Lorentz averaging parameter is $\Delta=2$ MeV.

Having a closer look at the full strengths in Fig. 1, we see still some differences between SkT6, SkM*, SLy6 and SkI3 cases. There is a small shift of the average peak position as well as different strength patterns. The most prominent peculiarities can be explained by the isovector parameters listed in Table 1. For example, the exceptionally large collective shift in SkM* can be related to very low isovector effective mass $m_1^*/m=0.65$ for this force or, which is the same, to a high value of the sum rule enhancement factor $\kappa=0.531$. It is seen that this case drastically deviates from the SkT6 one where the impact of the isovector parameters is negligible ($m_1^*/m=1.0$ and $\kappa=0.001$).

The trend of the average peak position devotes a special analysis. It can be related to the isovector parameters in the combination $\sqrt{a_{\text{sym,act}}/m_1^*}$ where $a_{\text{sym,act}} \approx a_{\text{sym}} - a'_{\text{sym}}\rho_{\text{nm}}/2$ is an estimate for the actual symmetry energy in a heavy nucleus and the density $\rho_{\text{nm}}/2$ at the nuclear surface determines the GDR response. This predicts the sequence of the peak heights with the highest SkM*, smaller SLy6 and lowest SkT6 and SkI3, in agreement with

Fig. 1. Note that this explanation takes care of the “actual” symmetry energy whose trend deviates from the trend of the volume symmetry energy a_{sym} (which then delivers the wrong trend in macroscopic estimates of the GDR peak [10]).

The detailed pattern of the strength distributions is caused by the fragmentation of the bulk dipole peak over energetically close 2qp states. Fig. 1 shows that the spectral details considerably vary with the force. This is best visible for SkM* case where unrealistically high right GDR shoulder and the subsequent overestimation of the resonance width take place, especially in ^{150}Nd . The effect becomes weaker for SLy6 (thus giving the best description of GDR) and vanishes for SkI3 (already with underestimation of the resonance width). The appearance of the right shoulder for some Skyrme forces, preferably those with a large effective mass, was also noted in the calculations for deformed rare-earth and actinide nuclei within the full (non-separable) Skyrme RPA [8] and in the SRPA calculations for ^{208}Pb [11]. This effect seems to be universal for GDR in heavy nuclei, independently on their shape.

The right shoulder of the GDR is studied in more detail in Fig. 2. To provide a more detailed description, we use here a smaller averaging of $\Delta = 1$ MeV. The left panels of the figure show the two GDR branches with projections $\mu = 0$ and $\mu = 1$. It is seen that the right shoulder effect is not caused by the deformation splitting since it appears only in the branch with $\mu = 1$. Instead, it is rather a consequence of the strength fragmentation. Following Fig. 2a, the branch $\mu = 1$ undergoes a dramatic transformation from SkM* to SkI3: its strength flows from the right to the left flank. To understand such behavior, we should take into account that the *unperturbed* dipole strength also has some kind of a right shoulder or a strong right tail (see Fig. 1) and this may cause a considerable fragmentation. The SkM* produces a maximal collective shift and thus places most of the $\mu = 1$ strength beyond the tail. This minimizes the fragmentation and collects the strength into the narrow peak. Vice versa, the SkI3 collective shift is small and insufficient to push the strength beyond the tail. So in this case the strength is fragmented between nearby 2qp pairs and we do not observe anymore large concentration of strength at the upper end of the spectrum.

It is interesting to figure out which single-particle states are responsible for the right flank of GDR. A simple analysis shows that these are the occupied intruder states $j = l + 1/2$ with the largest orbital momentum l . These sub-shells dive into the valence shell due to the strong spin-orbit splitting and, the heavier the nucleus, the stronger their impact. In ^{150}Nd , the intruder sub-shells are $1g_{9/2}$ for protons and $1h_{11/2}$ for neutrons. In ^{238}U , they are $1h_{11/2}$

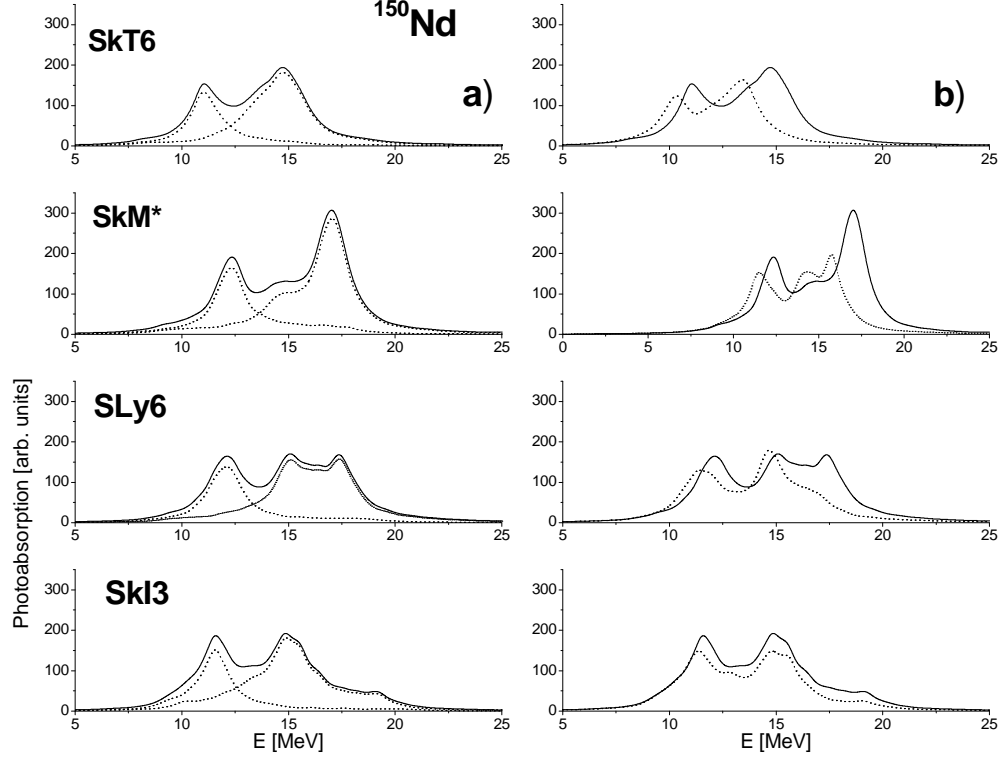


FIG. 2: The dipole giant resonance in ^{150}Nd and ^{238}U , calculated with the Skyrme forces SkT6, SkM*, SLy6 and SkI3. Plots a) exhibit the full strength (solid curve) and its branches $\mu = 0$ (left dotted structure) and $\mu = 1$ (right dotted structure). Plots b) exhibit the full strength with (solid curve) and without (dotted curve) the contribution from the proton sub-shell $1g_{9/2}$ and the neutron sub-shell $1h_{11/2}$. The Lorentz averaging parameter is $\Delta=1$ MeV.

and $1i_{13/2}$, respectively. Fig. 2b shows that excluding these sub-shells indeed weakens the right flank of GDR. It worth noting that such sub-shells should manifest themselves in GDR of heavy nuclei independently of the nuclear shape. The same effect appears in spherical heavy nuclei as well.

As a next step, we consider the influence of time-odd densities in the residual interaction. Following our calculations, only the current-current contribution $\delta^2 E / \delta \vec{j}_{s1} \delta \vec{j}_s$ is essential, while contributions related with the spin density are negligible. So, we will discuss only the effect of the current-current term $\sim (b_1 + b'_1 \delta_{s,s'})$. Fig. 3 shows that the time-odd contribution strongly depends on the force and, moreover, obviously correlates with the differences in strength distributions presented in Fig. 1. This is not surprising since the squared current density is involved to the terms $\sim b_1, b'_1$ of the Skyrme functional and just the time-even

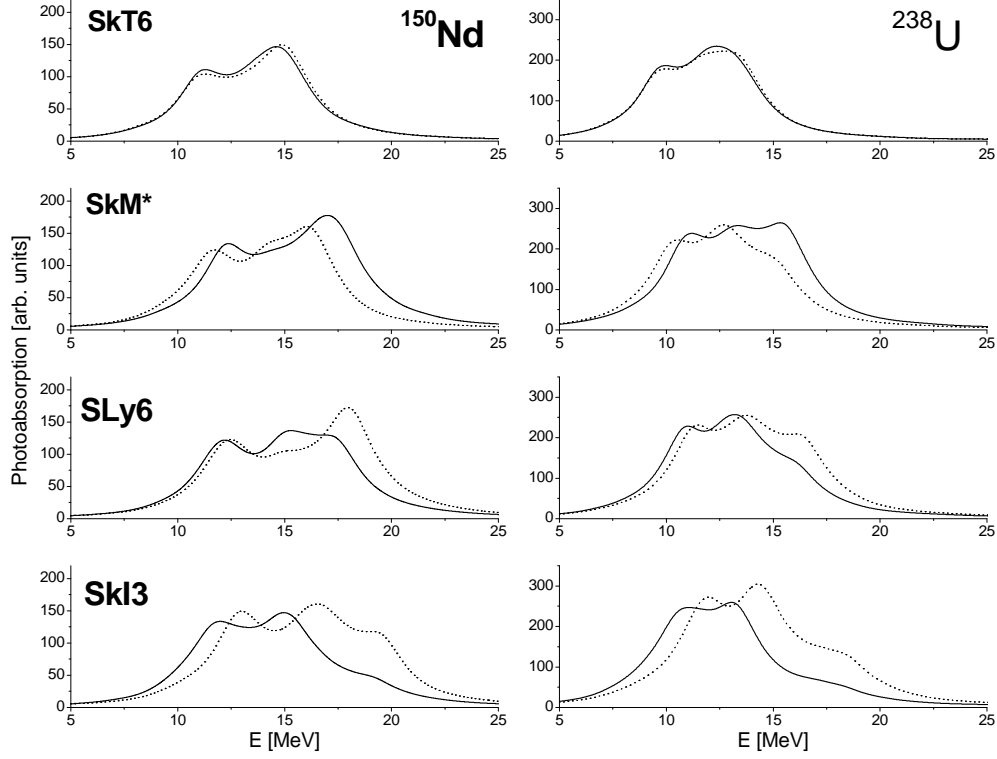


FIG. 3: The dipole giant resonance in ^{150}Nd and ^{238}U , calculated with the Skyrme forces SkT6, SkM*, SLy6 and SkI3. The full strength is calculated with (solid curve) and without (dashed curve) the current contribution. The Lorentz averaging parameter is $\Delta=2$ MeV.

partners in this term are responsible for the effective masses, see Eq. (2). As is seen from the figure, the time-odd effect is negligible for SkT6 (where $m_0^*/m = m_1^*/m = 1$ and thus the influence of the effective masses is minimal) but quite strong for other forces. Besides, the effect may have different sign (compare SkM* versus SLy6 and SkI3). The surprisingly large influence of the time-odd terms (and of the effective mass) can be understood by the fact that the dominant contributions to the dipole response from the principle Skyrme terms have different signs and thus considerably compensate each other [12]. Hence small effects, like the time-odd terms, acquire more weight.

It is remarkable, that the time-odd densities and effective masses affect the same part of GDR, namely its right flank. As was shown above, this part of the resonance strictly depends on the intruder states with a high orbital moment. Such states should be very sensitive to any velocity dependent values and hence to the current and effective masses. Then it is clear why just the right GDR flank is mainly affected by these values. This property of the GDR can be effectively used for additional testing the isovector parameters.

Altogether, we see that the average peak position is basically determined by the isovector parameters (symmetry energy, isoscalar effective mass) while the detailed fragmentation pattern is also strongly influenced by the isoscalar effective mass. A systematic analysis of dipole strength distribution over many spherical and deformed nuclei will help us to learn more about the underlying single particle spectra and dynamics.

IV. CONCLUSIONS

The giant dipole resonance (GDR) in deformed nuclei has been investigated within the separable RPA (SRPA) method. Four different Skyrme forces (SkT6, SkM*, SLy6, and SkI3) with different nuclear matter characteristics (symmetry energy, isoscalar and isovector effective mass) were applied. As the test cases, the typical axially deformed nuclei, ^{150}Nd and ^{238}U , were considered. SRPA was found to provide a good description of the GDR and, what is important, with a minimal computational effort. This method is indeed an efficient theoretical tool for systematic exploration of the dynamics of deformed nuclei.

All four Skyrme forces in our sample reproduce in general the average position of the GDR strength and its two-bump structure. There are some trends in the peak positions (shifts about ± 1 MeV) which can be explained by the different isovector properties of the forces. At closer inspection, we see considerable differences in the GDR width and fragmentation pattern. For example, some forces as, e.g., SkM* result in a too high right shoulder of the GDR strength distribution. We show that height and position of this shoulder are determined by high-angular-momentum states which are shifted down into the valence shell by the strong spin-orbit force. Thus many factors (effective mass, spin-orbit force) have a significant influence on the fragmentation pattern of the spectra, especially at the right flank of the GDR. This feature, in turn, provides useful information for determination of the Skyrme parameters and exploration of the possible correlations.

We have also discussed the effect of the time-odd terms on the GDR profile. The time-odd spin-orbit terms have only negligible influence. The current-current coupling, however, contributes substantially, and the lower the isoscalar effective mass, the stronger the contribution. This effect is crucial to counterweight the spectral stretching of the unperturbed excitations.

As we have seen, the detailed pattern of the resonance spectra carry worthwhile informa-

tion on the underlying single-particle spectrum of the self-consistent mean field. The newly developed SRPA code for deformed nuclei provides access to a much larger pool of data on nuclear giant resonances. This allows more systematic investigations to disentangle various influences and improve description of nuclear excitation properties. Work in that direction is in progress.

Acknowledgements

The work was supported by the DFG grant GZ:436 RUS 17/104/05, Heisenberg-Landau (Germany-BLTP JINR) grants for 2005 and 2006 years, and the BMBF, contracts 06 DD 119 and 06 ER 808, and by the research plan MSM 0021620834 of Czech Republic.

-
- [1] T.H.R. Skyrme, *Phil. Mag.* **1**, 1043 (1956).
 - [2] D. Vauterin, D.M. Brink, *Phys. Rev.* **C5**, 626 (1972).
 - [3] Y.M. Engel, D.M. Brink, K. Goeke, S.J. Krieger, and D. Vauterin, *Nucl. Phys.* **A249**, 215 (1975).
 - [4] J. Dobaczewski and J. Dudek, *Phys. Rev.* **C52**, 1827 (1995).
 - [5] M. Bender, P.-H. Heenen, and P.-G. Reinhard, *Rev. Mod. Phys.* **75**, 121 (2003).
 - [6] M.V. Stoitsov, J. Dobaczewski, W. Nazarewicz, S. Pittel, and D.J. Dean, *Phys. Rev.* **C68**, 054312 (2003).
 - [7] A. Obertelli, S. Peru, J.-P. Delaroche, A. Gillibert, M. Girod, and H. Goutte, *Phys. Rev.* **C71**, 024304 (2005).
 - [8] J.A. Maruhn, P.-G. Reinhard, P.D. Stevenson, J. Rikovska Stone, and M.R. Strayer, *Phys. Rev.* **C71**, 064328 (2005).
 - [9] P.-G. Reinhard, *Nucl. Phys.* **A649**, 305c (1999).
 - [10] G.F. Bertsch and R.A. Broglia, *Oscillations in Finite Quantum Systems* (Cambridge University Press, Cambridge, 1994).
 - [11] V.O. Nesterenko, J. Kvasil, and P.-G. Reinhard, *Phys. Rev.* **C66**, 044307 (2002).
 - [12] V.O. Nesterenko, W. Kleinig, J. Kvasil, P.-G. Reinhard, and P. Vesely, ArXiv: nucl-th/0609018; submitted to *Phys. Rev. C*.

- [13] V.O. Nesterenko, J. Kvasil, W. Kleinig, P.-G. Reinhard, and D.S. Dolci, ArXiv: nucl-th/0512045.
- [14] P.-G. Reinhard, *Ann. Phys. (Leipzig)* **1**, 632 (1992).
- [15] F. Tondeur, M. Brack, M. Farine, and J.M. Pearson, *Nucl. Phys.* **A420**, 297 (1984).
- [16] J. Bartel, P. Quentin, M. Brack, C. Guet, and H.-B. Håkansson, *Nucl. Phys.* **A386**, 79 (1982).
- [17] E. Chabanat, P. Bonche, P. Haensel, J. Meyer, and R. Schaeffer, *Nucl. Phys.* **A643**, 441(E) (1998).
- [18] P.-G. Reinhard and H. Flocard, *Nucl. Phys.* **A584**, 467 (1995).
- [19] A.S Goldhaber and G.S. Goldhaber, *Phys. Rev.* **C17**, 1171 (1978).
- [20] V.O. Nesterenko, V.P. Likhachev, P.-G. Reinhard, V.V. Pashkevich, W. Kleinig, and J. Mesa, *Phys. Rev.* **C70**, 057304 (2004).
- [21] JANIS database: 10025.029-0 (Sac1971).
- [22] S.S. Dietrich and B.L. Bergman, *At. Data Nucl. Data Tables* **38**, 199 (1998); IAEA Photonuclear Data.